

Ferrimagnetic long-range order caused by periodicity of exchange interactions in the spin-1 trimer chain compounds $\text{ANi}_3\text{P}_4\text{O}_{14}$ ($A = \text{Ca}, \text{Sr}, \text{Pb}, \text{Ba}$)

Masashi Hase,* Hideaki Kitazawa, Naohito Tsujii, Kiyoshi Ozawa, Masanori Kohno, and Giyuu Kido
National Institute for Materials Science (NIMS), 1-2-1 Sengen, Tsukuba 305-0047, Japan

(Received 24 February 2006; revised manuscript received 19 June 2006; published 31 July 2006)

We report magnetic properties of $\text{ANi}_3\text{P}_4\text{O}_{14}$ ($A = \text{Ca}, \text{Sr}, \text{Pb}, \text{Ba}$). A spin-1 trimer chain with J_1 - J_1 - J_2 interactions exists, where J_1 and J_2 denote two exchange interaction parameters. A magnetic phase transition occurs and a small spontaneous magnetization appears at low temperatures. The temperature dependence of magnetic susceptibility above the transition temperature and the magnetic-field dependence of magnetization in high magnetic fields are consistent with quantum Monte Carlo results for a spin model that consists of trimer chains with antiferromagnetic J_1 and ferromagnetic J_2 interactions. The small spontaneous magnetization is explainable qualitatively by ferrimagnetic long-range order in the chains and by imperfect cancellation of the net magnetic moments of the chains. To our knowledge, this is the first observation of ferrimagnetic long-range order whose origin is the periodicity of the exchange interactions in chains.

DOI: [10.1103/PhysRevB.74.024430](https://doi.org/10.1103/PhysRevB.74.024430)

PACS number(s): 75.10.Jm, 75.50.Gg, 75.30.Cr

I. INTRODUCTION

Studies on low-dimensional quantum spin systems have contributed greatly to our understanding of quantum mechanics. In particular, one-dimensional quantum spin systems have been studied widely for a long time because quantum-mechanical effects are conspicuous and because accurate theoretical results are obtainable. As a result, we realize that one-dimensional quantum spin systems show various magnetic properties. Magnetic long-range order is unstable even at 0 K because of strong quantum fluctuations. The ground state and low-lying excitations depend on the spin value in Heisenberg antiferromagnetic (AF) uniform chains. The ground state is the quantum-disordered (spin-liquid) state and the magnetic excitation is gapless in the spin-1/2 Heisenberg AF uniform chain. The ground state is a kind of ordered state with a string order parameter and a spin gap exists in magnetic excitations when the spin value is an integer.¹

Heisenberg AF bond-alternating chains have also been investigated extensively. A spin gap appears in spin-1/2 Heisenberg AF bond-alternating chains with $0 < \delta \leq 1$, where the two exchange interaction parameters are defined as $J(1 \pm \delta)$.² The spin-Peierls transition is a phase transition from uniform to bond-alternating chains that can occur because of the magnetic energy gain arising from the bond alternation.^{3,4} In contrast, the spin gap disappears at a critical value $\delta_c \sim 0.25$ in spin-1 Heisenberg AF bond-alternating chains.⁵ The ground state is in the Haldane phase and a singlet-dimer phase for $\delta < \delta_c$ and $\delta > \delta_c$, respectively. In addition, a phenomenon called the magnetization plateau can appear in magnetic fields.⁶⁻¹⁰

Recently, trimer and tetramer chains have attracted much attention because they show interesting magnetism that originates from the periodicity in the chains. Magnetization plateaus can appear in trimer and tetramer chains irrespective of the spin value.¹¹ It has been demonstrated experimentally¹² that the spin-1/2 trimer chain compound $\text{Cu}_3(\text{P}_2\text{O}_6\text{OH})_2$ has a 1/3 magnetization plateau and that the spin-1/2 tetramer chain compounds $\text{Cu}(\text{3-chloropyridine})_2(\text{N}_3)_2$

(Ref. 13) and $(\text{CH}_3)_2\text{NH}_2\text{CuCl}_3$ (Ref. 14) have a 1/2 magnetization plateau. Quantum ferrimagnetism caused by periodicity of exchange interactions is a unique phenomenon; it cannot occur in uniform and bond-alternating chains. The compound $\text{Cu}(\text{3-chloropyridine})_2(\text{N}_3)_2$ has a spin-1/2 tetramer chain with ferromagnetic-ferromagnetic-antiferromagnetic-antiferromagnetic interactions. The product of the magnetic susceptibility and temperature reaches a minimum around 10 K, followed by a steep increase upon further cooling. This temperature dependence suggests that $\text{Cu}(\text{3-chloropyridine})_2(\text{N}_3)_2$ is a quantum ferrimagnet. Ferrimagnetic long-range order can appear if interchain exchange interactions exist. However, experimental observations have not been reported so far.

Very recently, we recognized that the insulating compounds $\text{ANi}_3\text{P}_4\text{O}_{14}$ ($A = \text{Ca}, \text{Sr}, \text{Pb}, \text{Ba}$) can have spin-1 trimer chains as shown by their crystal structures.¹⁵⁻¹⁹ We observed that small spontaneous magnetizations appeared at low temperatures. We can explain the experimental result qualitatively using ferrimagnetic long-range order in the chains and imperfect cancellation of the net magnetic moments of the chains. To our knowledge, this paper reports the first observation of ferrimagnetic long-range order that is caused by the periodicity of exchange interactions in chains.

II. EXPECTED SPIN SYSTEM IN $\text{ANi}_3\text{P}_4\text{O}_{14}$ ($A = \text{Ca}, \text{Sr}, \text{Pb}, \text{Ba}$)

The crystal structures of $\text{ANi}_3\text{P}_4\text{O}_{14}$ ($A = \text{Ca}, \text{Sr}, \text{Pb}, \text{Ba}$) are identical. The space group is $P2_1/c$ (no. 14). As described below, we measured x-ray diffraction and calculated lattice constants. The lattice constants are summarized in Table I. Only the Ni^{2+} ions have spin 1. The positions of Ni and O connecting to Ni are shown schematically in Fig. 1. Two crystallographic Ni sites [Ni(1) and Ni(2)] exist along with two kinds of short Ni-Ni bonds. For example, in $\text{SrNi}_3\text{P}_4\text{O}_{14}$, Ni-Ni the distances in the first-shortest and second-shortest bonds (bonds 1 and 2), which are indicated, respectively, as bold and thin bars, are 3.14 and 3.23 Å. The

TABLE I. Ion radii of divalent ions, lattice constants, Ni-Ni distances, Ni-O-Ni angles, magnetic phase transition temperature T_F , and spin-flop field H_{SF} of $\text{ANi}_3\text{P}_4\text{O}_{14}$ ($A=\text{Ca, Sr, Pb, Ba}$).

		Ca	Sr	Pb	Ba	
Ion radius (\AA)		0.99	1.12	1.20	1.34	
a (\AA)		7.330	7.407	7.402	7.526	
b (\AA)		7.589	7.658	7.673	7.779	
c (\AA)		9.398	9.440	9.468	9.573	
β (deg)		112.1	112.2	112.4	112.8	
Structure	Bond 1	Ni-Ni (\AA)	3.11	3.14	3.15	3.19
		Ni-O-Ni (deg)	93.6	93.5	93.8	93.9
	Bond 2	Ni-Ni (\AA)	3.21	3.23	3.22	3.27
		Ni-O-Ni (deg)	102.6	102.7	102.4	102.7
Bond 3	Ni-Ni (\AA)	4.70	4.72	4.73	4.77	
	T_F (K) in 0.01 T	15.8	15.3	15.6	14.5	
Magnetism	H_{SF} (T) at 2 K	2.2	3.5	3.9	5.0	

first-shortest Ni-Ni bond has two Ni-O-Ni paths. The Ni-O-Ni angles in the two paths are 93.5° and 100.6° . It is noteworthy that the center of the two Ni sites in the first-shortest bond is an inversion center. The second-shortest Ni-Ni bond has two identical Ni-O-Ni paths whose angle is 102.7° . From the Ni-Ni distances and Ni-O-Ni angles, exchange interactions are expected to exist in the first-shortest and second-shortest Ni-Ni bonds. The respective parameters of their interactions are defined as J_1 and J_2 . The signs of J_1 and J_2 , however, cannot be judged from the crystal structure because the Ni-O-Ni angles are close to 90° . We will discuss

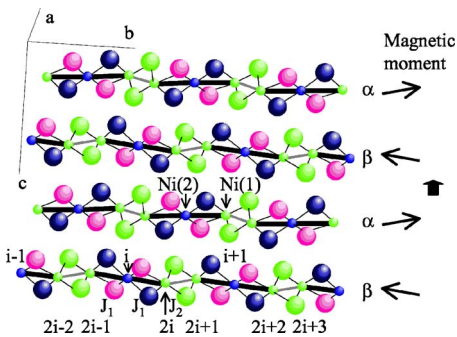


FIG. 1. (Color online) Schematic drawing of positions of Ni and O connecting to Ni in $\text{ANi}_3\text{P}_4\text{O}_{14}$ ($A=\text{Ca, Sr, Pb, Ba}$). Small and large circles denote Ni and O sites, respectively. Bold and thin bars represent the first-shortest and second-shortest Ni-Ni bonds, respectively. A spin-1 trimer (J_1 - J_1 - J_2) chain exists. Its Hamiltonian is expressed as $\mathcal{H}=\sum_i J_1 S(1)_{2i-1} S(2)_i + J_1 S(2)_i S(1)_{2i} + J_2 S(1)_{2i} S(1)_{2i+1}$, where $S(1)_j$ and $S(2)_i$ are the spin-1 operators at the $\text{Ni}(1)_j$ and $\text{Ni}(2)_i$ sites, respectively. Although all the trimer chains are identical as spin systems, there are two kinds of chains α and β , because of the difference in local orientations of nearest-neighbor Ni-Ni bonds. Thin and bold arrows show schematically the net magnetic moment of each chain and the total moment in the ordered phase. We do not determine the actual directions of the net magnetic moment of each chain and the total moment in this study.

the signs of J_1 and J_2 later. In contrast, a distance of Ni-Ni in the third-shortest bond (bond 3) is 4.72 \AA . Therefore, exchange interactions in the other bonds are probably weaker than the J_1 and J_2 interactions. As is shown in Table I, the other compounds have similar Ni-Ni distances and Ni-O-Ni angles.²⁰

As a result, it is considered that spin-1 trimer (J_1 - J_1 - J_2) chains parallel to the b direction mainly determine the magnetic properties of these compounds. Of course, as is the case of many Ni^{2+} compounds, single-ion anisotropy might affect the magnetic properties. All the trimer chains in each compound are identical as spin systems. From the viewpoint of local orientation of nearest-neighbor Ni-Ni bonds, however, two kinds of chains exist: α and β . The orientations of bonds 1 and 2 in the α chains are not parallel to those in the β chains. The numbers of the two chains are equal.

III. METHODS OF EXPERIMENTS AND CALCULATION

A crystalline powder of $\text{ANi}_3\text{P}_4\text{O}_{14}$ ($A=\text{Ca, Sr, Pb, Ba}$) was synthesized using the solid-state reaction method in air for 150 h with intermediate grindings. The sintering temperatures are 1273, 1273, 1173, and 1173 K for $A=\text{Ca, Sr, Pb, Ba}$, respectively. We used x-ray diffraction measurement to confirm the formation of $\text{ANi}_3\text{P}_4\text{O}_{14}$. Other materials could not be detected in the powder samples of $\text{SrNi}_3\text{P}_4\text{O}_{14}$ and $\text{PbNi}_3\text{P}_4\text{O}_{14}$. Very weak peaks of $\text{Ni}_3\text{P}_2\text{O}_8$ and $\text{BaNi}_2\text{P}_2\text{O}_8$ were observed in the powder samples of $\text{CaNi}_3\text{P}_4\text{O}_{14}$ and $\text{BaNi}_3\text{P}_4\text{O}_{14}$, respectively. $\text{Ni}_3\text{P}_2\text{O}_8$ (Ref. 21) and $\text{BaNi}_2\text{P}_2\text{O}_8$ (Ref. 22) show antiferromagnetic long-range order without spontaneous magnetization below 17.1 and 23.5 K, respectively.

We measured the magnetization M up to the magnetic field $H=5$ T using a superconducting quantum interference device (SQUID) magnetometer produced by Quantum Design. High-field magnetizations up to $H=30$ T were measured using an extraction-type magnetometer in a hybrid magnet at the High Magnetic Field Center, NIMS. We mixed the $\text{ANi}_3\text{P}_4\text{O}_{14}$ powders and paraffin, unified them by melting the paraffin, and used the unified sample for SQUID measurement. We used pressed pellets of $\text{ANi}_3\text{P}_4\text{O}_{14}$ powders for the high-field magnetization measurement. Thus, alignment of the powders was unchanged in the magnetization measurements.

We calculated the susceptibility and magnetization of spin-1 trimer chains by quantum Monte Carlo (QMC) techniques using the loop algorithm²³ and using the directed-loop algorithm in the path-integral formulation,²⁴ respectively. The numbers of Ni sites are 120 and 48 for calculations of the susceptibility and magnetization, respectively. We performed more than 1×10^6 updates. Finite-size effects and statistical errors are negligible in the scale of the figures represented in this paper.

IV. EXPERIMENTAL RESULTS

Figure 2(a) shows the temperature T dependence of M/H of $\text{ANi}_3\text{P}_4\text{O}_{14}$ ($A=\text{Ca, Sr, Pb, Ba}$) below 20 K measured in $H=0.01$ T. The dots and solid curves, respectively, represent

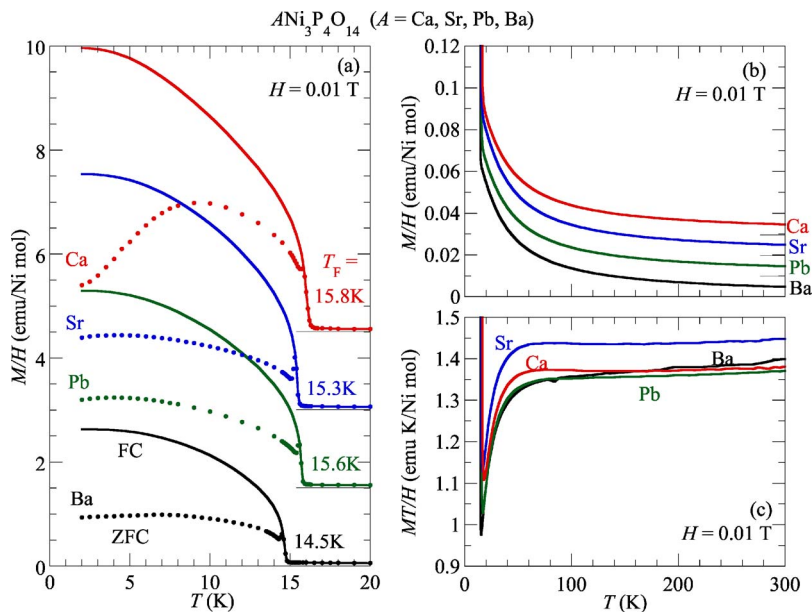


FIG. 2. (Color online) (a) The temperature dependence of M/H of $ANi_3P_4O_{14}$ ($A = \text{Ca, Sr, Pb, Ba}$) below 20 K measured in $H = 0.01$ T. The dots and solid curves indicate magnetization measured in zero-field-cooling and field-cooling processes, respectively. Vertical positions of M/H for $A = \text{Ca, Sr, and Pb}$ are shifted, respectively, by 4.5, 3.0, and 1.5 emu/Ni mol. (b) The temperature dependence of M/H below 300 K measured in $H = 0.01$ T. The vertical positions of M/H for $A = \text{Ca, Sr, and Pb}$ are shifted, respectively, by 0.03, 0.02, and 0.01 emu/Ni mol. (c) The temperature dependence of MT/H below 300 K measured in $H = 0.01$ T.

M/H measured in zero-field-cooling (ZFC) and field-cooling (FC) processes. First, we explain the M/H curves of $SrNi_3P_4O_{14}$ as representative. A sharp peak appears at 15.3 K in the ZFC process, and temperature hysteresis is clearly visible below the same temperature. These results indicate occurrence of a magnetic phase transition at $T_F = 15.3$ K. The magnitude of M/H increases rapidly on cooling below about 16 K, indicating that magnetic long-range order with spontaneous magnetization appears below T_F . In the ordered phase, M/H in the ZFC process shows a broad peak at around 4.5 K and M/H in the FC process increases monotonically on cooling. Similar magnetic properties are observed in $ANi_3P_4O_{14}$ ($A = \text{Ca, Pb, Ba}$), but a sharp peak at T_F and a broad peak in the ZFC process in the ordered phase are, respectively, less and more evident in $CaNi_3P_4O_{14}$. The values of the transition temperature T_F are 15.8, 15.6, and 14.5 K for $A = \text{Ca, Pb, and Ba}$; they are described in Table I.

Figure 2(b) shows the T dependence of M/H below 300 K in $H = 0.01$ T. Because the maximum of the vertical axis is 0.12, Fig. 2(b) cannot show M/H at low T . On cooling, M/H increases following the Curie-Weiss law from 300 K. We fitted the formula $C/(T + \theta) + \chi_0$ to the experimental M/H above 100 K. Here, C , θ , and χ_0 represent the Curie constant, Weiss temperature, and a constant term of the susceptibility. The evaluated values of the fitting parameters are well known to depend on the temperature region used in the fitting. For that reason, we were unable to determine values of the fitting parameters uniquely, but the evaluated values of C and χ_0 are close to expected values. As for θ , both positive and negative values are possible. We can say, however, that the magnitude of θ is small (a few kelvins or less) in comparison with the transition temperatures. Figure 2(c) shows the T dependence of MT/H below 300 K in $H = 0.01$ T. The values of MT/H are almost constant at high T and are then reduced at temperatures less than about 60 K. These reductions indicate that one or more dominant exchange interactions in each compound are antiferromagnetic.²⁵

Figure 3(a) shows the H dependence of the magnetization of $ANi_3P_4O_{14}$ ($A = \text{Ca, Sr, Pb, Ba}$) at 2 K measured using

the SQUID magnetometer. Hysteresis of the magnetization curves is readily visible at low magnetic fields. For example, the slope of the magnetization above 3.5 T is slightly greater than that below 3.5 T in $SrNi_3P_4O_{14}$. Similar behaviors are observed for the other compounds. This change of the slope probably indicates a spin-flop transition. Because a rapid increase of the magnetization attributable to the spin-flop transition is apparent only in H parallel to ordered moments, the increase is weakened in magnetization of the powder sample. We describe the estimated values of the fields of the spin-flop transition in Table I.

The solid curves of Fig. 3(b) show H dependence of the magnetization at 1.7 K up to 30 T measured using the extraction-type magnetometer. The magnetization is almost saturated at 30 T. The small residual magnetization indicates that the spontaneous magnetization is small. Because the direction of residual magnetic fields is opposite to that of the applied magnetic fields, the initial magnetization is negative.²⁶

V. DISCUSSION

Let us consider the mechanism of the appearance of the small spontaneous magnetization. As described above, the signs of J_1 and J_2 cannot be determined from the crystal structure. Therefore, four kinds of spin models that consist of trimer chains are possible from the signs of J_1 and J_2 . We examined whether the four spin models can explain the experimental results or not; we subsequently concluded that only the AAF model shown below could account for the experimental results.

We consider a spin model that consists of spin-1 trimer (J_1 - J_1 - J_2) chains with antiferromagnetic J_1 and ferromagnetic J_2 interactions. We name it the AAF model. If magnetic long-range order is stabilized where spins in each chain are aligned collinearly by the J_1 and J_2 interactions, the spins on the Ni(1) sites are parallel to one another, the spins on the Ni(2) sites are parallel to one another, and the Ni(1) spins are

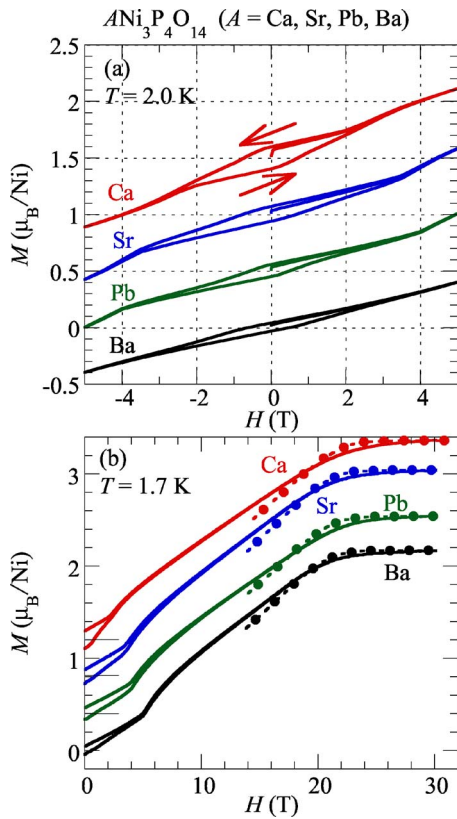


FIG. 3. (Color online) (a) The magnetic-field dependence of M of $\text{ANi}_3\text{P}_4\text{O}_{14}$ ($A=\text{Ca, Sr, Pb, Ba}$) at 2 K measured by the SQUID magnetometer. The arrows denote the direction of the change of H . The vertical positions of M for $A=\text{Ca, Sr, and Pb}$ are shifted, respectively, by $1.5, 1.0,$ and $0.5\mu_{\text{B}}/\text{Ni}$. (b) The magnetic-field dependence of M at 1.7 K measured by the extraction-type magnetometer (solid curves) and the QMC results of M (dashed curves) for the AAF model with $J_1=10$ K and $J_2=-125$ K for Ca and Sr and $J_1=9.6$ K and $J_2=-120$ K for Pb and Ba. Because the solid and dashed curves overlap with each other above 20 T, the dashed curves cannot be seen clearly. The circles represent some points of the QMC results. We draw these circles in order to indicate that two curves exist. Because the experimental data are powder averages of magnetizations in the ordered phase, the AAF model cannot reproduce the experimental data in low H . Thus, the calculated magnetizations below 14 T are not shown. The vertical positions of M for $A=\text{Ca, Sr, and Pb}$ are shifted, respectively, by $1.2\mu_{\text{B}}, 0.8\mu_{\text{B}},$ and $0.4\mu_{\text{B}}$ per Ni.

antiparallel to the Ni(2) spins. The Ni(1) sites are twice as numerous as the Ni(2) sites. For that reason, each chain shows ferrimagnetism and has a net magnetic moment whose value is about $(2/3)\mu_{\text{B}}/\text{Ni}$. The experimental residual magnetic moments, however, are only $0.1\mu_{\text{B}}/\text{Ni}$ or less. If the directions of the net moments of the chains are the same in each domain and if the directions of the net moments of the domains are random, the residual magnetic moment is roughly estimated as $2/3 \times 1/2 = 1/3\mu_{\text{B}}/\text{Ni}$. Here, the factor $1/2$ comes from the azimuthal average of the net moments of the domains that are randomly aligned. Consequently, the small residual magnetic moments indicate that the net moments of the chains cancel one another imperfectly. As described previously, two kinds of chains exist: α and β . The

orientations of the bonds 1 and 2 in the α chains are not parallel to those in the β chains. The small residual magnetic moments can remain if the direction of the net magnetic moment of the chain α deviates a little from the opposite direction of the net magnetic moment of the chain β . The speculated magnetic structure is shown schematically in Fig. 1. Probably, single-ion anisotropy of the Ni^{2+} spins has a greater influence on the spin structure in the ordered phase than interchain interactions and causes the above-mentioned deviation of the moment directions. To our knowledge, the magnetic order in $\text{ANi}_3\text{P}_4\text{O}_{14}$ ($A=\text{Ca, Sr, Pb, Ba}$) is the first example of ferrimagnetic long-range order that is caused by the periodicity of the exchange interactions in the chains.

We compared the experimental results with QMC results for the AAF model. Because the experimental magnetizations have a characteristic structure, the onset of saturation around 22 T, we compared first the experimental magnetizations with calculated magnetizations. We calculated the magnetization for several values of $j \equiv J_1/J_2$. In each calculated magnetization curve, values of J_1 and J_2 were determined in order that the calculated curve was close to the experimental curve in high magnetic fields. Next, we calculated susceptibilities for the values of J_1 and J_2 determined above, compared the calculated susceptibility curves with the experimental M/H curves above T_{F} , and chose a calculated curve that could reproduce the experimental curve best in each compound. As a result, we estimate that $J_1=10$ K and $J_2=-125$ K for the Ca and Sr compounds and that $J_1=9.6$ K and $J_2=-120$ K for the Pb and Ba compounds. The value of j is -0.08 in all the compounds. The dashed curves in Fig. 3(b) show the calculated magnetizations. The experimental and calculated magnetizations in high magnetic fields coincide with each other. Figure 4 shows the temperature dependence of the inverse susceptibility. In comparison between the experimental and calculated data, we added constant terms of the susceptibility with reasonable values (order of 10^{-4} emu/Ni mol) to the calculated susceptibilities. The calculated inverse susceptibilities indicated by dashed curves are consistent with the experimental H/M above T_{F} . Consequently, the AAF model can reproduce magnetic properties of $\text{ANi}_3\text{P}_4\text{O}_{14}$ ($A=\text{Ca, Sr, Pb, Ba}$) in high magnetic fields or above T_{F} . In our calculations, however, we did not take the single-ion anisotropy and interchain exchange interactions into account. It is difficult to perform calculations for models including all the interactions and to determine uniquely values of all the interactions because we have only the magnetization data. Thus, we may have to consider that the above-mentioned values of J_1 and J_2 are roughly estimated values. Values of J_1 and J_2 are probably altered by introduction of the single-ion anisotropy and interchain exchange interactions. Therefore, the result that the estimated values of J_1 are comparable to the values of T_{F} does not mean necessarily that the trimer chain model is inadequate to explain the magnetic properties of $\text{ANi}_3\text{P}_4\text{O}_{14}$ ($A=\text{Ca, Sr, Pb, Ba}$).

Here, we estimate errors of J_1 and J_2 in the case that we consider only the J_1 and J_2 interactions. In comparison between the experimental and calculated magnetizations, estimated values of J_1 are close to 10 K for all j . Therefore, the

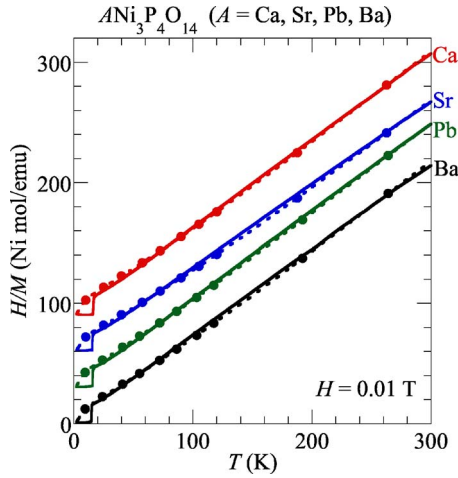


FIG. 4. (Color online) The temperature dependence of H/M of $\text{ANi}_3\text{P}_4\text{O}_{14}$ ($A=\text{Ca, Sr, Pb, Ba}$) measured in $H=0.01$ T (solid curves) and the QMC results of inverse susceptibility (dashed curves) for the AAF model with $J_1=10$ K and $J_2=-125$ K for Ca and Sr and $J_1=9.6$ K and $J_2=-120$ K for Pb and Ba. Because the solid and dashed curves overlap with each other, the dashed curve cannot be seen clearly. The circles represent some points of the QMC results. We draw these circles in order to indicate that two curves exist. In the calculated curves, constant terms of susceptibilities are included. Values of the constant terms are 2, 1, 3, and 2×10^{-4} emu/Ni mol. The vertical positions for $A=\text{Ca, Sr, and Pb}$ are shifted, respectively, by 90, 60, and 30 Ni mol/emu.

error of J_1 is small. The result that values of J_1 are almost independent of j means that the value of the saturation field is mainly determined by the antiferromagnetic J_1 interaction. In the Ca and Sr compounds, calculated susceptibilities with $j=-0.06$ and $J_2=-165$ K or $j=-0.10$ and $J_2=-100$ K differ a little from the experimental ones. Similarly, in the Pb and Ba compounds, calculated susceptibilities with $j=-0.06$ and $J_2=-160$ K or $j=-0.10$ and $J_2=-95$ K differ a little from the experimental ones. Thus, we estimated the range of J_2 as -165 to -100 K for Ca and Sr and -160 to -95 K for Pb and Ba. We have to estimate values of J_2 from the M/H data above T_F , which have monotonic temperature dependence. Accordingly, the errors of J_2 are not small.

Next, we consider a spin model that consists of spin-1 trimer ($J_1-J_1-J_2$) chains with ferromagnetic J_1 and J_2 interactions. We name it the FFF model. Each chain can have a spontaneous magnetization. The FFF model, however, cannot explain magnetism of $\text{ANi}_3\text{P}_4\text{O}_{14}$ ($A=\text{Ca, Sr, Pb, Ba}$) for the following reason. Because the residual magnetizations are small, interchain exchange interactions are antiferromagnetic. If the effect of the interchain exchange interactions is more dominant than that of the single-ion anisotropy, the spin structure in the ordered phase must be collinear. Collinear spin structures caused by AF interchain interactions, however, cannot have spontaneous magnetizations. Thus, the magnitude of the single-ion anisotropy (usually the D term) is inferred to be larger than that of the interchain interactions. The values of the spin-flop field ($2 \sim 5$ T) and saturation field (above 20 T) reflect the magnitudes of the single-ion anisotropy and AF interchain interactions, respectively. Therefore, from the experimental magnetizations, the

magnitude of the single-ion anisotropy is expected to be smaller than that of the interchain interactions, which is inconsistent with the above-mentioned inference. Consequently, the spin system in $\text{ANi}_3\text{P}_4\text{O}_{14}$ ($A=\text{Ca, Sr, Pb, Ba}$) is not the FFF model. In addition, as was described, the decrease of MT/H on cooling shown in Fig. 2(c) indicates that one or more dominant exchange interactions in each compound are antiferromagnetic. This result is not consistent with the FFF model, because the AF interchain interactions are expected to be small.

Finally, we consider the remaining two spin models. One model consists of spin-1 trimer ($J_1-J_1-J_2$) chains with antiferromagnetic J_1 and J_2 interactions; it is named the AAA model. The other consists of trimer chains with ferromagnetic J_1 and antiferromagnetic J_2 interactions; it is named the FFA model. When only the J_1 and J_2 interactions are taken into account, two spins on $\text{Ni}(1)_{2i}$ and $\text{Ni}(1)_{2i+1}$ sites are antiparallel to each other. Also, two spins on $\text{Ni}(2)_i$ and $\text{Ni}(2)_{i+1}$ sites are antiparallel to each other. The center of the $\text{Ni}(1)_{2i}$ and $\text{Ni}(1)_{2i+1}$ sites is the inversion center. Therefore, it is quite natural to consider that the magnitudes of the magnetic moments of the $\text{Ni}(1)$ spins are the same and that the magnitudes of the magnetic moments of the $\text{Ni}(2)$ spins are the same. Consequently, the spontaneous magnetizations cannot be generated only by the J_1 and J_2 interactions even if the magnitudes of the magnetic moments of the $\text{Ni}(1)$ and $\text{Ni}(2)$ spins differ from each other.

We consider the possibility that the spontaneous magnetizations are caused by introduction of the anisotropy. In Ni^{2+} ions, the origins of the anisotropy are the single-ion anisotropy and the Dzyaloshinsky-Moriya (DM) interaction. Because the center of the $\text{Ni}(1)_{2i}$ and $\text{Ni}(1)_{2i+1}$ sites is the inversion center, the easy axes of the spins on these two $\text{Ni}(1)$ sites are antiparallel to each other; furthermore, the easy axes of the spins on $\text{Ni}(2)_i$ and $\text{Ni}(2)_{i+1}$ sites are antiparallel to each other. Therefore, the single-ion anisotropy does not change the situation that the $\text{Ni}(1)_{2i}$ and $\text{Ni}(1)_{2i+1}$ spins are antiparallel to each other and the situation that the $\text{Ni}(2)_i$ and $\text{Ni}(2)_{i+1}$ spins are antiparallel to each other. The DM interaction does not exist between the $\text{Ni}(1)_{2i}$ and $\text{Ni}(1)_{2i+1}$ spins because of the inversion center. The DM interaction, in contrast, might exist between the $\text{Ni}(2)_i$ and $\text{Ni}(1)_{2i}$ spins. For those reasons, the $\text{Ni}(2)_i$ and $\text{Ni}(1)_{2i}$ spins might become noncollinear. The DM vector between the $\text{Ni}(2)_i$ and $\text{Ni}(1)_{2i}$ spins is antiparallel to that between the $\text{Ni}(2)_{i+1}$ and $\text{Ni}(1)_{2i+1}$ spins because of the inversion center. Therefore, the $\text{Ni}(2)_i$ and $\text{Ni}(2)_{i+1}$ spins are antiparallel to each other even if the DM interaction exists between the $\text{Ni}(2)_i$ and $\text{Ni}(1)_{2i}$ spins. As a result, the single-ion anisotropy and DM interaction can cause no spontaneous magnetization.

VI. CONCLUSION

We measured the temperature and magnetic-field dependence of magnetization of $\text{ANi}_3\text{P}_4\text{O}_{14}$ ($A=\text{Ca, Sr, Pb, Ba}$). Two kinds of Ni^{2+} sites exist and form a spin-1 trimer chain with $J_1-J_1-J_2$ interactions, where J_1 and J_2 denote two kinds of exchange interaction parameters. We observed a magnetic

phase transition and small spontaneous magnetization at low temperatures. The temperature dependence of magnetic susceptibility above the transition temperature and the magnetic-field dependence of magnetization in high magnetic fields are consistent with QMC results for a spin model that consists of trimer chains with antiferromagnetic J_1 and ferromagnetic J_2 interactions. The small spontaneous magnetization is explainable qualitatively by ferrimagnetic long-range order in the chains and by imperfect cancellation of the net magnetic moments of the chains. To our knowledge, this observation is the first of ferrimagnetic long-range order caused by the periodicity of the exchange interactions in the chains. In future studies, the spin structure in the ordered

phase should be determined by neutron-diffraction measurements.

ACKNOWLEDGMENTS

We are grateful to S. Matsumoto for syntheses of samples and x-ray diffraction measurements, to H. Mamiya and H. Sakurai for invaluable discussion, and to M. Kaise for x-ray diffraction measurements. This work was supported by grants for basic research from NIMS and by a Grant-in-Aid for Scientific Research from the Ministry of Education, Culture, Sports, Science, and Technology.

*Electronic address: HASE.Masashi@nims.go.jp

- ¹T. Kennedy and H. Tasaki, *Commun. Math. Phys.* **147**, 431 (1992).
- ²J. C. Bonner, S. A. Friedberg, H. Kobayashi, D. L. Meier, and H. W. J. Blöte, *Phys. Rev. B* **27**, 248 (1983).
- ³J. W. Bray, H. R. Hart Jr., L. V. Interrante, I. S. Jacobs, J. S. Kasper, G. D. Watkins, S. H. Wee, and J. C. Bonner, *Phys. Rev. Lett.* **35**, 744 (1975).
- ⁴M. Hase, I. Terasaki, and K. Uchinokura, *Phys. Rev. Lett.* **70**, 3651 (1993); M. Hase, I. Terasaki, Y. Sasago, K. Uchinokura, and H. Obara, *ibid.* **71**, 4059 (1993); M. Hase, I. Terasaki, K. Uchinokura, M. Tokunaga, N. Miura, and H. Obara, *Phys. Rev. B* **48**, 9616 (1993); M. Hase, N. Koide, K. Manabe, Y. Sasago, K. Uchinokura, and A. Sawa, *Physica B* **215**, 164 (1995); M. Hase, K. Uchinokura, R. J. Birgeneau, K. Hirota, and G. Shirane, *J. Phys. Soc. Jpn.* **65**, 1392 (1996).
- ⁵R. R. P. Singh and M. P. Gelfand, *Phys. Rev. Lett.* **61**, 2133 (1988).
- ⁶T. Tonegawa, T. Nakao, and M. Kaburagi, *J. Phys. Soc. Jpn.* **65**, 3317 (1996).
- ⁷K. Totsuka, *Phys. Lett. A* **228**, 103 (1997).
- ⁸Y. Narumi, M. Hagiwara, R. Sato, K. Kindo, H. Nakano, and M. Takahashi, *Physica B* **246**, 509 (1998).
- ⁹Y. Narumi, K. Kindo, M. Hagiwara, H. Nakano, A. Kawaguchi, K. Okunishi, and M. Kohno, *Phys. Rev. B* **69**, 174405 (2004).
- ¹⁰M. Hase, M. Kohno, H. Kitazawa, O. Suzuki, K. Ozawa, G. Kido, M. Imai, and X. Hu, *Phys. Rev. B* **72**, 172412 (2005).
- ¹¹K. Hida, *J. Phys. Soc. Jpn.* **63**, 2359 (1994).
- ¹²M. Hase, M. Kohno, H. Kitazawa, N. Tsujii, O. Suzuki, K. Ozawa, G. Kido, M. Imai, and X. Hu, *Phys. Rev. B* **73**, 104419 (2006).
- ¹³M. Hagiwara, Y. Narumi, K. Minami, K. Kindo, H. Kitazawa, H. Suzuki, N. Tsujii, and H. Abe, *J. Phys. Soc. Jpn.* **72**, 943 (2003).
- ¹⁴Y. Inagaki, A. Kobayashi, T. Asano, T. Sakon, H. Kitagawa, M. Motokawa, and Y. Ajiro, *J. Phys. Soc. Jpn.* **74**, 2683 (2005).
- ¹⁵A. P. Dindune, V. V. Krasnikov, and Z. A. Konstant, *Izv. Akad. Nauk SSSR, Neorg. Mater.* **20**, 1553 (1984) [*Inorg. Mater.* **20**, 1335 (1984)]; V. V. Krasnikov, Z. A. Konstant, and V. K. Bel'skii, *ibid.* **21**, 1560 (1985) [**21**, 1360 (1985)].
- ¹⁶K.-H. Lii, P.-F. Shih, and T.-M. Chen, *Inorg. Chem.* **32**, 4373 (1993).
- ¹⁷A. Elmarzouki, A. Boukhari, A. Berrada, and E. M. Holt, *J. Solid State Chem.* **118**, 202 (1995).
- ¹⁸M. Bolte, *Acta Crystallogr.* **E57**, i30 (2001).
- ¹⁹B. El-Bali, A. Boukhari, J. Aride, K. Maaß, D. Wald, R. Glaum, and F. Abraham, *Solid State Sci.* **3**, 669 (2001).
- ²⁰Atomic positions in $\text{BaNi}_3\text{P}_4\text{O}_{14}$ have not been determined yet. We tried to refine structure parameters by the Rietveld method from x-ray diffraction data of $\text{BaNi}_3\text{P}_4\text{O}_{14}$ using the RIETAN program [F. Izumi and T. Ikeda, *Mater. Sci. Forum* **321-324**, 198 (2000)]. Agreement factors in our refinement, however, were not so good. Therefore, we calculated Ni-Ni distances and Ni-O-Ni angles of $\text{BaNi}_3\text{P}_4\text{O}_{14}$ using the atomic positions in $\text{SrNi}_3\text{P}_4\text{O}_{14}$ and using the lattice constants of $\text{BaNi}_3\text{P}_4\text{O}_{14}$, because x-ray diffraction patterns of $\text{ANi}_3\text{P}_4\text{O}_{14}$ ($A=\text{Ca, Sr, Pb, Ba}$) are similar to one another. The Ni-Ni distances and Ni-O-Ni angles of $\text{BaNi}_3\text{P}_4\text{O}_{14}$ calculated using the data of $\text{SrNi}_3\text{P}_4\text{O}_{14}$ are almost the same as those using the data of $\text{CaNi}_3\text{P}_4\text{O}_{14}$ or $\text{PbNi}_3\text{P}_4\text{O}_{14}$.
- ²¹J. Escobal, J. L. Pizarro, J. L. Mesa, J. M. Rojo, B. Bazan, M. I. Arriortua, and T. Rojo, *J. Solid State Chem.* **178**, 2626 (2005).
- ²²L. P. Regnault, J. Rossat-Mignod, J. Y. Henry, and L. J. de Jongh, *J. Magn. Magn. Mater.* **31-34**, 1205 (1983).
- ²³See references in H. G. Evertz, *Adv. Phys.* **52**, 1 (2003).
- ²⁴O. F. Syljuåsen and A. W. Sandvik, *Phys. Rev. E* **66**, 046701 (2002).
- ²⁵In Ref. 16, the magnetic susceptibility of $\text{SrFe}_3\text{P}_4\text{O}_{14}$ measured in $H=0.5$ T is reported. The susceptibility increases rapidly below 26 K on cooling; this temperature dependence is similar to those at low T in $\text{ANi}_3\text{P}_4\text{O}_{14}$ ($A=\text{Ca, Sr, Pb, Ba}$). In our opinion, the existence of a magnetic phase transition was not confirmed in Ref. 16.
- ²⁶We performed electron-spin resonance measurements using an X-band spectrometer (JEOL-JES-RE3X) at room temperature. As is the case of many Ni^{2+} compounds, signals of the resonance from Ni^{2+} spins are too weak to determine the g factor.